



ELSEVIER

journal homepage: www.elsevier.com/locate/jmatprotec

Modeling influence of basic operation parameters on plasma jet

Fan Qunbo*, Wang Lu, Wang Fuchi

School of Material Science and Engineering, Beijing Institute of Technology, Beijing 100081, China

ARTICLE INFO

Article history:

Received 24 November 2006

Received in revised form 5 June 2007

Accepted 1 July 2007

Keywords:

Plasma spray

Operation parameters

Temperature field

Velocity field

Species distribution

ABSTRACT

In plasma spray, operation parameters, including current, flow rate of primary gas, and flow rate of secondary gas, would influence the heat and acceleration status of particles greatly, thus influencing the coating's final quality. As the first stage to optimize the spraying technology, this paper investigates the typical Ar–He plasma spray process, analyzing the influence mechanism of current, flow rate of Ar, as well as flow rate of He on the temperature field and velocity field. The chemical reactions and turbulence are fully taken into account. It is found that the electrical current is apparently influential to both the jet temperature and velocity, and further the ionization of Ar atoms. With increasing Ar or He flow rates independently, the temperature of the plasma jet will be decreased, and the velocity of the plasma jet will be increased. Related inner mechanisms are revealed in detail. The results presented in this paper would be theoretically helpful for further study of the interaction between the plasma jet and the particles, and the optimization of the plasma-spraying technology.

© 2007 Elsevier B.V. All rights reserved.

1. Introduction

In recent years, plasma spraying has become a widely acceptable technology in industry due to its variety of advantages, such as processing stability, the flexibility concerning size and shape of the samples to be coated, and low cost fabrication. Therefore, the optimization of plasma spraying has drawn much attention of researchers. In the spraying process, however, a high-temperature high-velocity jet, with violent and complex physical and chemical reactions, is produced, thus making the related research much more difficult (Chen, 1993; Lugscheider et al., 1996). In this case, numerical simulation can provide insight into phenomena that are either difficult to measure or that cannot to be directly measured.

With the fast development of software and hardware of computers, great achievements have been made, including

the optimization of turbulent model (Dussoubs et al., 1997), solving the complex chemical reactions of the mixture jet (Swank and Chang, 1992; George et al., 1996), analysis of three-dimensional heat transfer and flow (Dussoubs et al., 1997, 2001), and investigating the interaction between the high-temperature plasma jet and the ambient atmosphere (Chen, 1984; Leylavergne et al., 1998). Many researchers have reported that the quality of the sprayed coating mainly depends on the particles' heating and velocity history in the plasma jet. As the first stage to optimize the plasma-spraying technology, this paper systematically simulates the effect of basic operation parameters, electrical current, flow rates of primary and secondary working gases on the temperature field and the velocity field with respect to Ar–He plasma spraying. The interaction between the plasma jet and the particles, as well as the simulation of coating quality will be discussed by the author in future research reports.

* Corresponding author. Tel.: +86 10 8910 8185.

E-mail address: fanqunbo@bit.edu.cn (F. Qunbo).

0924-0136/\$ – see front matter © 2007 Elsevier B.V. All rights reserved.

doi:10.1016/j.jmatprotec.2007.07.008

2. Geometrical model and computational process

During the calculation, the following assumptions are made:

- (1) the plasma jet is a continuous media (Chen, 1993) in local thermodynamic equilibrium (Dussoubs et al., 1997; Nishiyama et al., 1998);
- (2) the plasma jet is composed of the primary gas Ar and secondary gas He, injecting into the ambient atmosphere;
- (3) the plasma jet is optically thin (Dussoubs et al., 1997; Nishiyama et al., 1998), ignoring the energy loss by radiation;
- (4) there is only one chemical reaction, $\text{Ar}^+ + e \leftrightarrow \text{Ar}$, ignoring the reaction of $\text{He}^+ + e \leftrightarrow \text{He}$ due to its relatively higher activation energy (Fan et al., 2004);
- (5) the plasma jet is in a steady state system (Dussoubs et al., 1997, 2001; Nishiyama et al., 1998).

As it can be seen that in Fig. 1, the geometrical model is in a 80 mm × 80 mm domain, where AB is located at the nozzle exit with the radius of 4 mm. Since the plasma gun and the plasma jet are axially symmetrical, a two-dimensional cylindrical model is employed. The origin of the coordinate is at the center of the nozzle exit, and the axial and radial coordinate are x and r , respectively. The computational domain is meshed into 80 × 50 elements, and in the radial direction the grid is more refined near the central axis and coarser towards the outer boundaries.

The boundary conditions at AB, including the initial velocity v_0 , the initial temperature T_0 , the initial turbulent kinetic energy K_0 , and the initial dissipation rate ε_0 , as well as the mass fraction of argon f_{Ar} , the mass fraction of argon ions f_{Ar^+} and the mass fraction of helium f_{He} , can be calculated by inputting the basic operation parameters (electrical current I , flow rates of argon F_{Ar} , and flow rates of helium F_{He}), and solving the energy conservation equations inside the plasma gun (Fan et al., 2004). The temperature and the pressure at other boundaries, BC, CD, DE, EF and FA, are 300 K and 1 atm, respectively; the initial mass fractions of f_{Ar} , f_{Ar^+} , f_{He} are assumed to be zero.

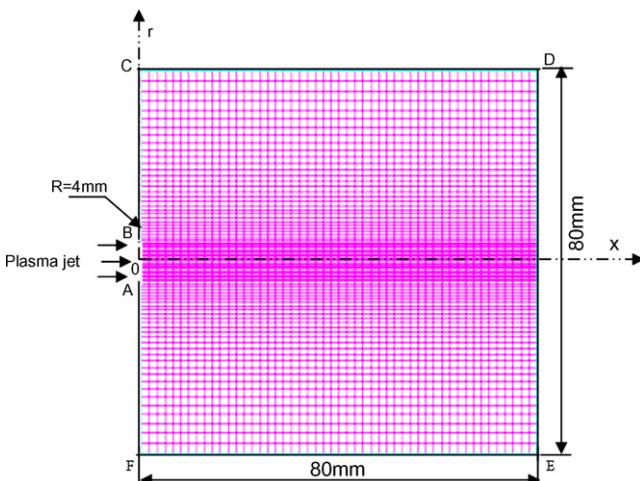


Fig. 1 – The calculation domain.

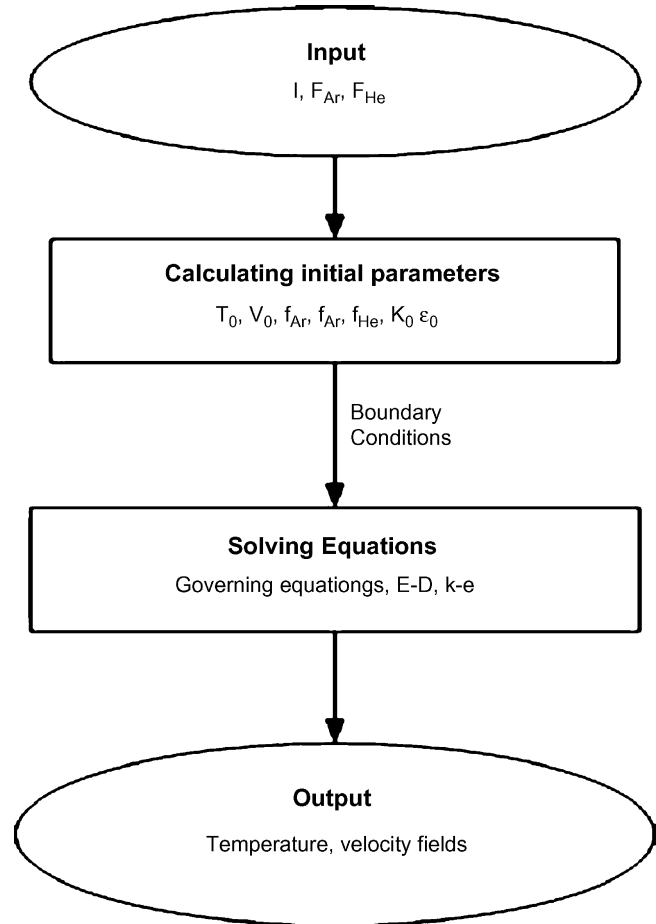


Fig. 2 – Flow chart of calculation.

Basic governing equations simulating the plasma jet include the mass conservation equation, the momentum conservation equation and the energy conservation equation (Chen and Fan, 1990); the classical turbulent $k-\varepsilon$ equations (Chen, 1984) to describe the turbulent kinetic energy and dissipation rate are also employed. In addition, the complex chemical reactions in the turbulent plasma jet shall be fully taken into account, which might be very difficult. To this end, the eddy-dissipation model (E-D model) (Magnussen and Hjertager, 1976) is solved, which successfully combines the reaction rates with the turbulent kinetic energy and dissipation rates of the reactants and products. All the equations above form a set of close equations. On the basis of the equations, if inputting the parameters I , F_{Ar} and F_{He} , the temperature field, velocity field can be output (see Fig. 2). All the calculation is conducted by using a commercial computational fluid dynamics package, FLUENT (Fluent, 1998).

3. Results and discussion

3.1. Influence of the electrical current I on the plasma jet

The temperature field, velocity field, Ar atom and Ar^+ ions concentrations under typical operation conditions ($F_{\text{Ar}} = 70 \text{ scf/h}$

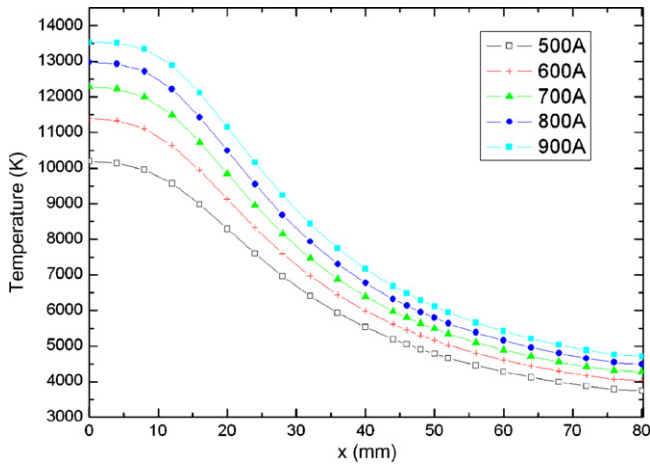


Fig. 3 – Distributions of temperature along the axis: with increasing electrical current, the temperature at the same positions will be increased.

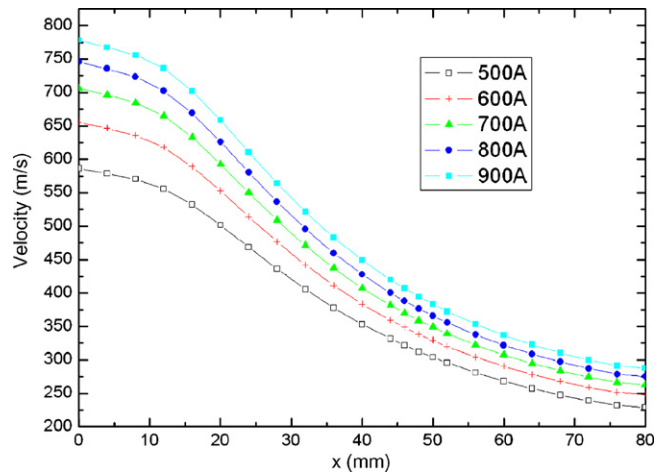


Fig. 4 – Distributions of velocity along the axis: with increasing electrical current, the velocity at the same positions will be increased.

and $F_{He} = 30 \text{ scf/h}$) are discussed in this section by inputting a serial of electrical currents: 500, 600, 700, 800 and 900 A.

3.1.1. *Influence of electrical current on temperature field*

Fig. 3 shows the temperature values along the axis under the serial of electrical currents. It can be seen that, the temperature filed in the plasma jet greatly depends on the electrical current. At the same position, the higher the electrical current I is, the higher the temperature is, which is directly related to the input power. Since the input power is proportional to the electrical current, increasing I will definitely increase the input power, thus raising the temperature of the whole plasma jet. It can also be seen, however, with increasing the axial distance, the temperature difference due to the different currents will become weakened. The main reason for this is that these regions have been far from the high-temperature and high-velocity jet core and the turbulent boundary layers.

3.1.2. *Influence of electrical current on velocity field*

Fig. 4 shows the distributions of velocity along the axis under a serial of currents. It can be seen from the figure that the influence of current on velocity is similar to the effect on temperature. At the same position, the relatively higher electrical current corresponds to relatively higher velocity, and with increasing the axial distances, such difference would be weakened. The high velocity of the plasma jet at the nozzle exit is due to the violent thermal expansion of the high-temperature plasma gas. Therefore, if the electrical current is increased, the temperature and the velocity of the plasma gas will be increased. But at those regions far from the plasma jet core and the turbulent boundary layers, this effect will become less and less apparent.

3.1.3. *Influence of electrical current on Ar and Ar⁺ distributions*

Fig. 5 shows the Ar and Ar⁺ concentration distributions along the axis under different currents. As seen in Fig. 5, the different

electrical currents do not influence the Ar atom concentration obviously, but it can still be found that a relatively higher electrical current causes a relatively lower Ar atom concentration. This is because a higher electrical current accelerates the decomposition reaction of Ar atoms. For the same reason, the concentration of Ar⁺ ions will increase with increasing electrical current, as can be seen in Fig. 6. However, with increasing axial distance, the Ar⁺ ions and electrons will recombine into Ar atoms. At about $x = 40 \text{ mm}$, the recombination reactions have ended.

3.2. *Influence of Ar flow rate on the plasma jet*

The temperature filed and velocity field under typical operation conditions ($I = 900 \text{ A}$ and $F_{He} = 30 \text{ scf/h}$) are discussed in this section by inputting a serial of Ar flow rates: 50, 60, 70, 80, and 90 scf/h.

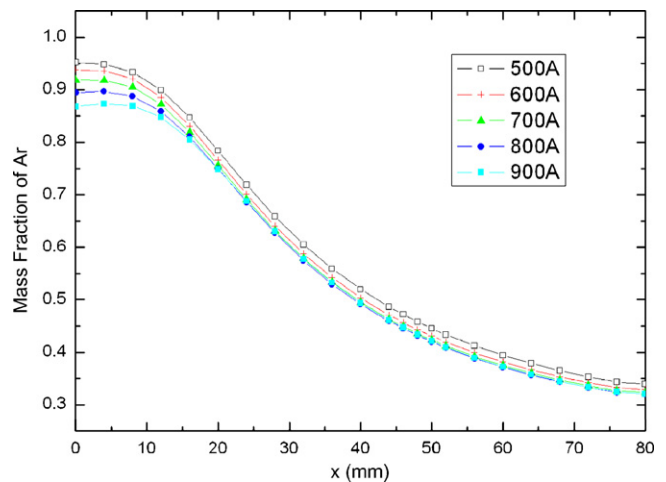


Fig. 5 – Distributions of Ar concentration along the axis: a relatively higher electrical current causes a relatively lower Ar atom concentration.

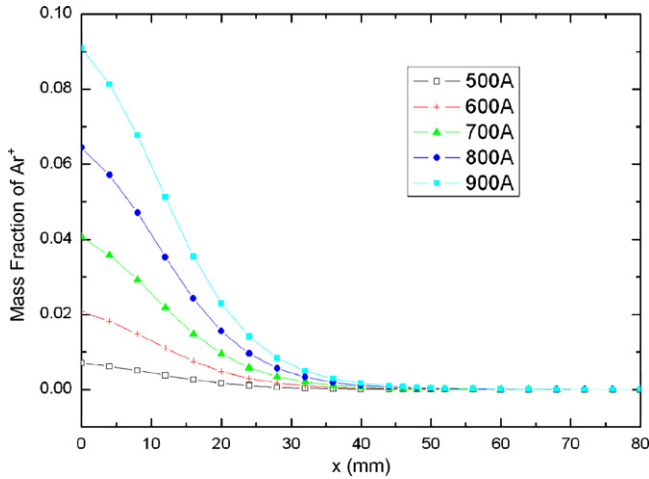


Fig. 6 – Distributions of Ar⁺ concentration along the axis for different currents: at about x = 40 mm, the Ar⁺ ion recombination reactions have ended.

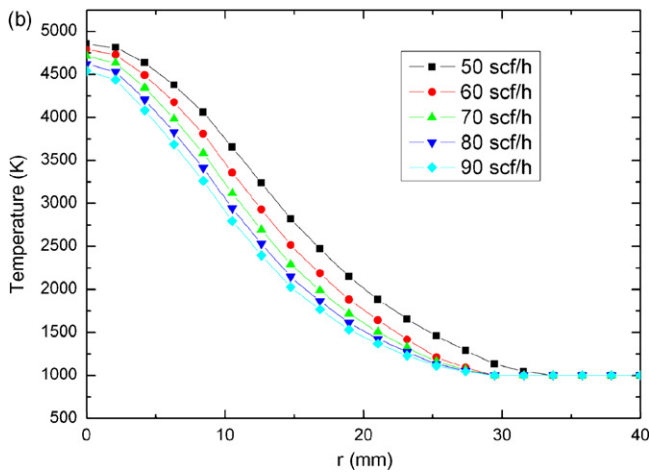
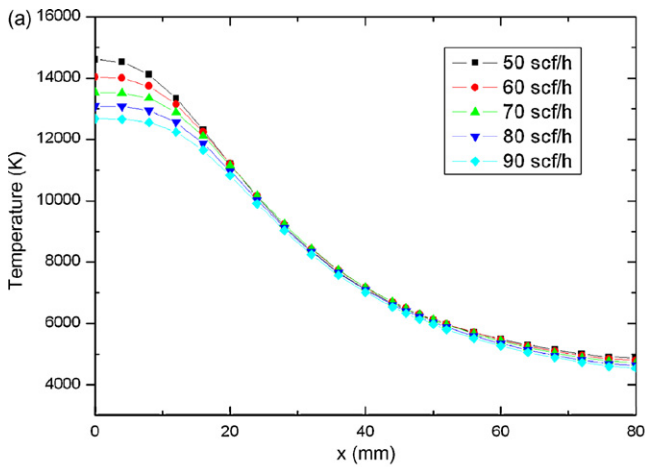


Fig. 7 – Distributions of temperature (a) along the axis (b) along the radial position (x = 80 mm) for different Ar flow rates: with increasing Ar flow rates, the temperature at the same positions will be decreased.

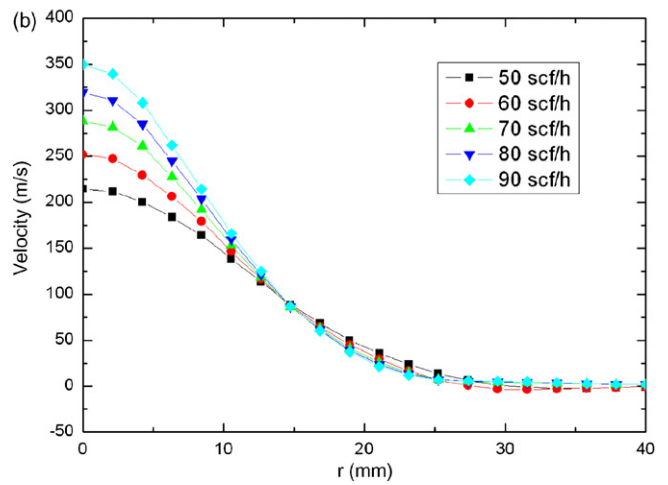
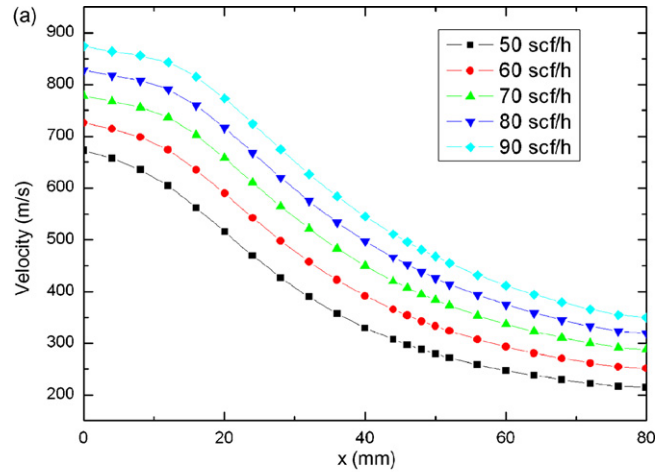


Fig. 8 – Distributions of velocity (a) along the axis (b) along the radial position (x = 80 mm) for different Ar flow rates: with increasing Ar flow rates, the velocity at the same positions will be increased.

3.2.1. Influence of Ar flow rate on the temperature field

Fig. 7(a) and (b) shows the temperature distributions along the axis and the radial position (x = 80 mm) respectively under different Ar flow rates. As is presented in Fig. 7(a), near the region of the plasma jet core, the higher the flow rate of Ar, lower the temperature is. But at the regions far from the plasma jet core (x > 20 mm), such influence will become weakened. At different radial positions (x = 80 mm), the temperature level has generally decreased. The highest temperature decreases to 4858 K, as seen in Fig. 7(b). Fig. 7(b) also shows that a higher primary gas flow rate causes a lower temperature at the same positions.

3.2.2. Influence of Ar flow rate on the velocity field

Fig. 8(a) and (b) present the velocity distributions along the axis and along the radial positions (x = 80 mm) under different Ar flow rates. As shown in Fig. 8(a), the Ar flow rate influences the velocities along the axis. The larger the Ar flow rate, the larger the velocity is, and with increasing axial distance, such difference does not become weakened apparently comparing

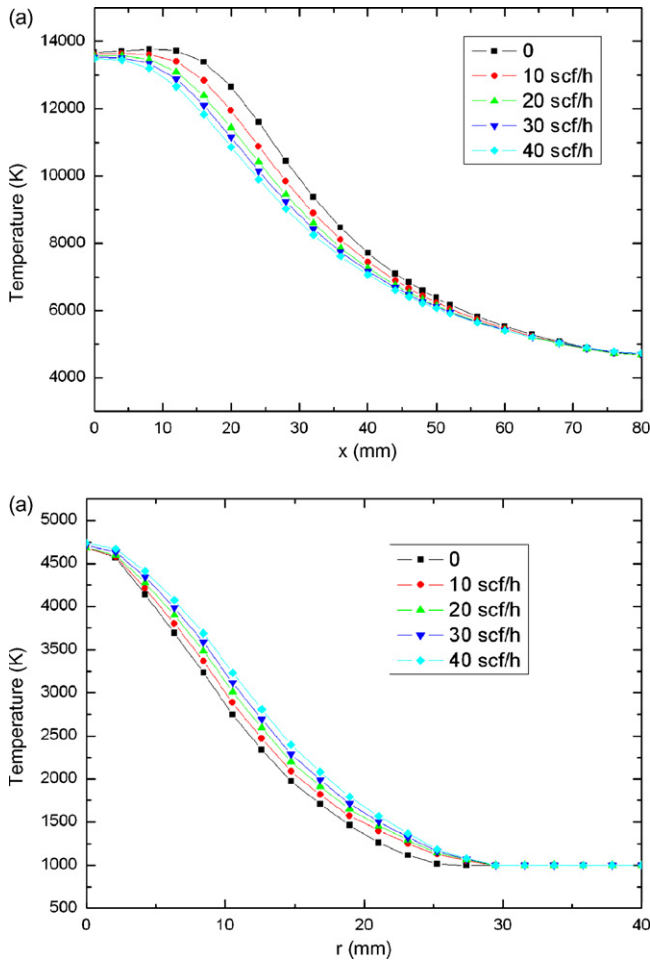


Fig. 9 – Distributions of temperature (a) along the axis (b) along the radial position ($x=80$ mm) for different He flow rates: with increasing He flow rates, the temperature at the same positions will be decreased, but the violent entrainment effect of the ambient air is found in radial positions.

with that of temperatures. In other words, the temperature at the inlet has less influence on the characteristics of the plasma jet, which is in good agreement with the conclusion drawn by literature (Zhang et al., 2007). But at $x=80$ mm, with increasing radial distance, the velocities of all the working conditions tends to be zero, as shown in Fig. 8(b).

When the electrical current and the flow rate of He are kept constant in plasma spraying, with increasing flow rate of Ar, the temperature near the nozzle exit is relatively lower. The reason for this is because the atom numbers in a unit volume will be correspondingly increased, but the total input power increases only slightly.

3.3. Influence of He flow rate on the plasma jet

The temperature field and velocity field under typical operation conditions ($I=900$ A and $F_{He}=30$ scf/h) are discussed in this section by inputting a serial of He flow rates: 0, 10, 20, 30, and 40 scf/h.

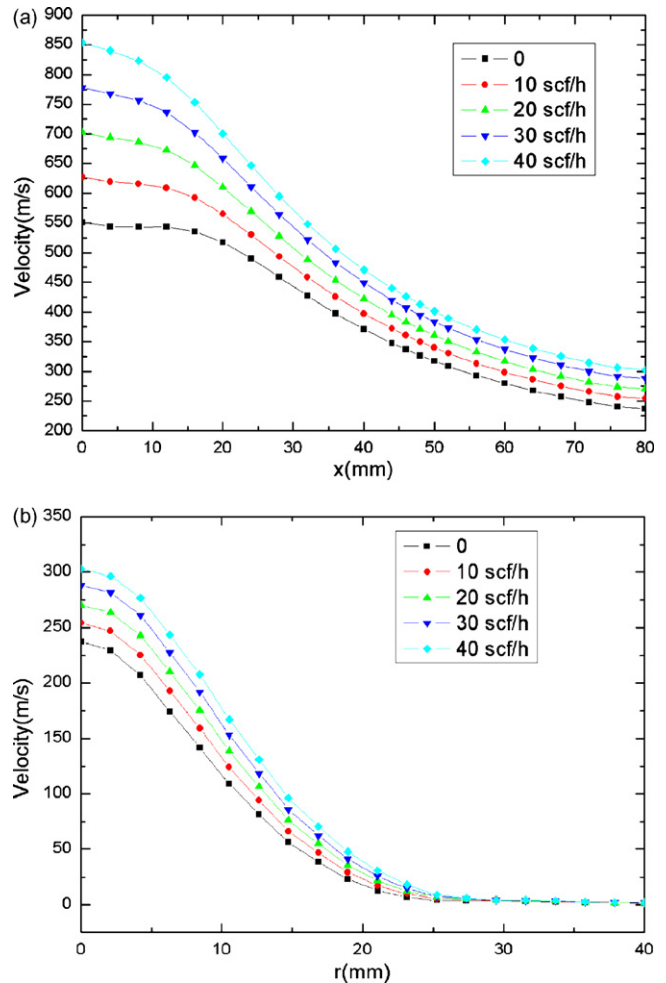


Fig. 10 – Distributions of velocity (a) along the axis (b) along the radial position ($x=80$ mm) for different He flow rates: with increasing He flow rates, the velocity at the same positions will be increased.

3.3.1. Influence of He flow rate on the temperature field

Fig. 9(a) and (b) shows the temperature distributions along the axis and along the radial positions ($x=80$ mm) under different He flow rates. As is shown in Fig. 9(a), at the same axial position, with increasing the He flow rate, the temperature of the plasma jet will be decreased due to the same reason as the primary gas Ar. As presented in Fig. 9(b), however, at the same radial positions less than 30 mm, a larger flow rate of He corresponds to a relatively higher temperature, which is the result of the violent entrainment effect of the ambient air penetrating into the plasma jet.

3.3.2. Influence of He flow rate on the velocity field

Fig. 10(a) and (b) shows the distributions of velocity along the axis and the radial position ($x=80$ mm) under different He flow rates. It can be seen from the figures that at the same axial or radial positions, with increasing flow rate of He, the velocity will be increased, though such effect will become weakened when far from the nozzle exit. It can also be found that the velocities along the radial positions descend much faster than that along the axis. When other operation parameters are kept

constant, the influence of He flow rate on the jet velocity is more apparent than that on the jet temperature, which is in good agreement with the experimental observations.

4. Conclusions

With respect to Ar-He plasma spraying, the influence of the electrical current, the flow rate of primary gas, as well as the flow rate of the secondary gas on the plasma jet are investigated, which would be helpful to further predict the interaction between the plasma jet and the flying particles, and optimize the plasma-spraying technology. The main conclusions are as follows:

- (1) The influence of the electrical current on the jet temperature and velocity is apparent. At the same positions, with increasing electrical current, both the temperature and the velocity will be increased. In addition, the ion degree of Ar atoms is dependent on the electrical current. A higher electrical current corresponds to a higher ion degree of Ar atoms.
- (2) The higher the flow rate of Ar, the higher the jet velocity at the same positions is. With increasing axial distance, the velocities will be decreased. Comparing with the influence on temperature of Ar flow rates, the velocity decreasing rates are relatively slow, though the initial temperature at the inlet has a less influence on the characteristics of the plasma jet.
- (3) The flow rate of the secondary gas He is influential both on the plasma temperature and on the velocity. In general, the influence on velocity would be relatively stronger. If the flow rate of He is increased, the velocity of the plasma jet will be increased and the temperature will be decreased. It has also been found that, in local radial regions, a higher flow rate of He corresponds to a higher temperature, which is the result of the violent interaction between the plasma jet boundary and the outside ambient air.

Acknowledgement

This support in part by the Commission of Science Technology and Industry for National Defense under grant number 9140A12020306BQ01 and the Excellent Young Teacher Foun-

ation of Beijing Institute of Technology under Contract 1040012040101 was acknowledged.

REFERENCES

- Chen, Y.C., 1984. Modeling work in thermal plasma process, PhD Thesis, University of Minnesota, USA.
- Chen, X., 1993. Heat Transfer and Flow of High-temperature Ionic Gas. Science Press, Beijing (in Chinese).
- Chen, K.F., Fan, J.R., 1990. Theory and Calculation of Engineering Gas-Solid Multiphase Flow. Zhejiang University Press, Hangzhou (in Chinese).
- Dussoubs, B., Fauchais, P., Vardelle, A., Vardelle, M., 1997. Computational analysis of a three-dimensional plasma spray jet. In: Proceedings of the XXIII International Conference on Phenomena in Ionized Gases (ICPIG), vol. 2, pp. 158-159.
- Dussoubs, B., Vardelle, A., Mariaux, G., Themelis, N.J., Fauchais, P., 2001. Modeling of plasma spraying of two powders. *J. Therm. Spray. Technol.* 1, 105-110.
- Fan, Q.B., Wang, L., Wang, F.C., 2004. Numerical simulation of basic parameters in plasma spray. *J. Beijing Inst. Technol.* 1, 80-84.
- Fluent, 1998. FLUENT 5.4, User's Guide, Fluent Inc., Lebanon.
- George, C., Pfender, E., Steffens, H.D., 1996. Numerical Simulation of a Multi-component Reacting flow in a Supersonic DC Torch Nozzle. *Thermal Spray: Practical Solutions for Engineering Problems*. ASM International, USA, pp. 595-602.
- Leylaverne, M., Vardelle, A., Dussoubs, B., Goubot, N., 1998. Comparison of plasma-sprayed coatings produced in argon or nitrogen atmosphere. *J. Therm. Spray. Technol.* 4, 527-536.
- Lugscheider, E., Barimani, C., Eckert, P., Eritt, U., 1996. Modeling of the APS plasma spray process. *Comput. Mater. Sci.* 7, 109-114.
- Magnussen, B.F., Hjertager, B.H., 1976. On mathematical models of turbulent combustion with special emphasis on soot formation and combustion. In: Proceedings of the 16th Symposium on Combustion, The Combustion Institute, USA, pp. 719-729.
- Nishiyama, H., Kuzuhara, M., Solonenko, O.P., Kamiyama, S., 1998. Numerical modeling of an impinging dusted plasma jet controlled by a magnetic field in a low pressure. *Thermal Spray: Meeting the Challenges of the 21st Century*, vol.1. ASM International, France, pp. 451-456.
- Swank, W.D., Chang, C.H., 1992. Computational fluid dynamics modeling of multicomponent thermal plasma. *Plasma Chem. Plasma Process.* 3, 299-325.
- Zhang, H., Hu, S., Wang, G., Zhu, J., 2007. Modeling and simulation of plasma jet by lattice Boltzmann method. *Appl. Math. Model.* 31, 1124-1132.